PCCP

COMMUNICATION

View Article Online
View Journal

Cite this: DOI: 10.1039/c9cp02997d

Received 28th May 2019,
Accepted 24th June 2019

DOI: 10.1039/c9cp02997d

rsc.li/pccp

Large volume liquid state scalar Overhauser dynamic nuclear polarization at high magnetic field†

Thierry Dubroca, *[a] Sungsool Wi,[a] Johan van Tol,[a] Lucio Frydman [ab] and Stephen Hill*[ac]

Dynamic Nuclear Polarization (DNP) can increase the sensitivity of Nuclear Magnetic Resonance (NMR), but it is challenging in the liquid state at high magnetic fields. In this study we demonstrate significant enhancements of NMR signals (up to 70 on ^{13}C) in the liquid state by scalar Overhauser DNP at 14.1 T, with high resolution (∼0.1 ppm) and relatively large sample volume (∼100 μL).

NMR spectroscopy is widely used for the study of structural and dynamical properties of molecules and materials. Unfortunately, its sensitivity is very low. DNP can increase NMR's sensitivity by orders of magnitude by transferring magnetization from electrons to nuclei.[1,2] In DNP, the sample is mixed with organic radicals containing unpaired electron spins. These spins are driven out of equilibrium by irradiating the sample mixture with microwaves matching the electron Larmor frequency at the associated magnetic field. Through electron-nuclear cross-relaxation processes, the initial large electron polarization is transferred to the nuclei of interest, which can lead to dramatic increases in the observed NMR signal. At high magnetic fields DNP is most efficient in the solid phase, where the solid effect, cross effect, or thermal mixing dominate the electron-nuclear polarization transfer.[3] Dissolution DNP, where the sample is first hyperpolarized in a frozen solution at low temperature and then rapidly melted so that it can be studied in the liquid phase, provides one route to sensitivity-enhanced solution state NMR.[4] However, its applications are limited to long-lived spin states. DNP is challenging to perform directly in the liquid state at high magnetic fields due to the unfavorable scaling of the polarization transfer efficiency. Resolving this challenge would enable measurement of NMR spectra with high resolution and high sensitivity, a goal of great importance, with scientific applications such as low concentration studies of small molecules (*e.g.*, natural products and metabolites) and their molecular dynamics. Loening *et al.*[5] showed significant enhancements on a variety of nuclei (^{19}F, ^{31}P, ^{13}C, ^{15}N) at moderate magnetic field (5 T). Meanwhile, the Prisner group[6–9] demonstrated the feasibility of performing liquid DNP at higher field (9.2 T) on ^{1}H (≈80× enhancements), though in nano-liter sample volumes accommodated inside a custom microwave resonator needed to achieve the high microwave magnetic (B_1) fields required to drive an otherwise inefficient Overhauser electron-nuclear polarization transfer. Liu *et al.*[10] demonstrated very high enhancements on ^{13}C (≈1000×) at moderate magnetic fields (3.35 T), while van Meerten *et al.*[11] demonstrated ^{1}H DNP (≈160× at 3.35 T) in a very low viscosity solvent (supercritical CO_2, with viscosity $\eta \approx 40$ μPa s^{-1}) with measured correlation times of 2–4 ps needed to overcome the inefficient polarization transfer between the radical and the ^{1}H on the molecules of interest, paving the way to high field liquid ^{1}H DNP. More recently, Yoon *et al.*[12] demonstrated that liquid DNP is possible (≈10× ^{1}H and ≈200× ^{31}P enhancements) at high magnetic field (9.2 T) without a resonator and, therefore, with moderate sample volumes (≈10 μL).

We have also recently demonstrated a large liquid DNP enhancement at high fields (14.1 T) for ^{31}P in a large volume (100 μL) sample of triphenylphosphine.[13] The present investigation expands on that work by demonstrating that large ^{13}C DNP enhancements of up to 70× can be achieved at high fields (14.1 T) *via* the scalar Overhauser effect in large volume (100 μL) solutions containing several target molecules, while also improving the resolution, with ≈0.1 ppm linewidths typical of modern NMR spectrometers. The measurements described here were performed using an in-house developed DNP spectrometer operating at 14.1 T (*i.e.* 600/150 MHz ^{1}H/^{13}C frequencies), employing a custom solution-state NMR probe coupled to a 395 GHz gyrotron source *via* a quasi-optical table.[13] Fig. 1 illustrates typical enhancements obtained with this system (see ESI† for details), as reported by the ratios of the ^{13}C NMR peak amplitudes observed

[a] NHMFL, 1800 E. Paul Dirac Dr, Tallahassee, FL 32310, USA. E-mail: dubroca@magnet.fsu.edu
[b] Dept. Chem. and Bio. Physics, Weizmann Institute, 76100 Rehovot, Israel
[c] Department of Physics, Florida State University, Tallahassee, Florida 32306, USA. E-mail: shill@magnet.fsu.edu

† Electronic supplementary information (ESI) available: Temperature calibration, ancillary NMR spectra and microwave magnetic field calculations. See DOI: 10.1039/c9cp02997d

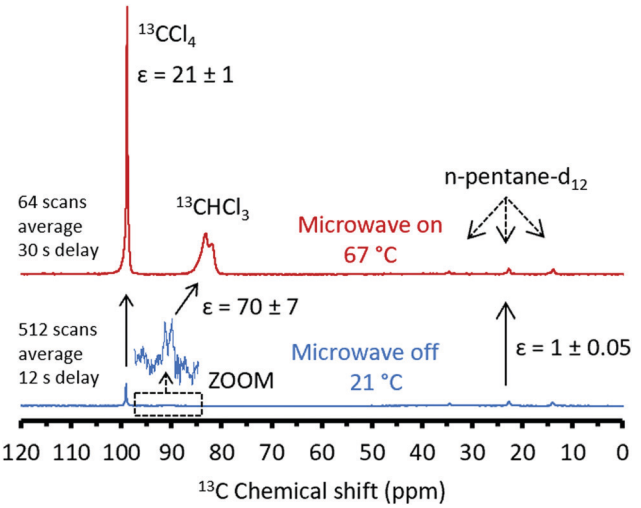

Fig. 1 ^{13}C NMR spectra of labelled CCl_4 and $CHCl_3$ measured at 14.1 T without (blue trace) and with microwaves (red trace). The CCl_4 linewidth remained essentially identical at 0.1 ppm. The natural abundance ^{13}C peaks from the solvent, *n*-pentane-d_{12}, are also visible. Sample information: $^{13}CCl_4$ (9% vol), $^{13}CHCl_3$ (1% vol, *i.e.* 125 mM) in *n*-pentane-d_{12} with 10 mM TEMPO (dissolved oxygen was removed by freeze pump thaw), 100 μL volume (3 mm OD, 2 mm ID and ~30 mm long sample tube). Microwave power: 13 W. Microwave gating time: 3 s before each NMR observation pulse (90°, no proton decoupling used).

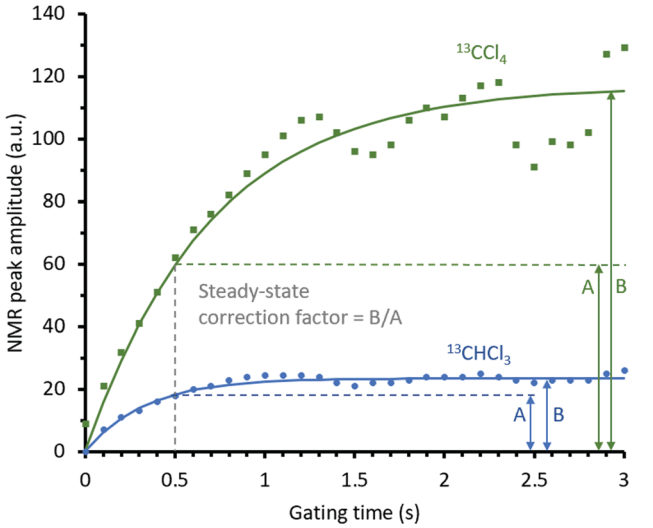

Fig. 2 ^{13}C NMR peak amplitude of labelled carbon tetrachloride (green squares) and chloroform (blue dots) measured at 14.1 T with increasing microwave gating time. The microwaves were on during the indicated times just prior to the NMR observation pulse. The solid lines are mono-exponential fits. The samples and experimental conditions were the same as those in Fig. 1. The parameter A marks the amplitude for a gating time of 0.5 s, while the parameter B marks the steady state amplitude. An average of 64 scans was used to collect each NMR spectrum.

with and without microwaves. These are ×21 ± 1 for $^{13}CCl_4$, and ×70 ± 7 for $^{13}CHCl_3$ in *n*-pentane-d_{12} with 10 mM TEMPO [(2,2,6,6-tetramethylpiperidin-1-yl)oxyl]; no enhancement are observed for the *n*-pentane-d_{12} peaks. As will be discussed later, these enhancements stem from scalar interactions of the nuclei under investigation with the unpaired electrons in the TEMPO radicals, which are absent for the ^{13}C of *n*-pentane. A significant rise in temperature during these experiments was observed due to microwave heating: from the change in the ^{13}C chemical shift of the $^{13}CHCl_3$ peak relative to $^{13}CCl_4$, we deduce that the temperature rose from 20 °C to 67 °C (see ESI,† Fig. SI-1, for details about the temperature calibration). This reflects the fact that the polar chloroform absorbs microwaves at 395 GHz;[14] a 125 mM concentration was employed to mitigate this heating. Also, to further reduce heating, the high power (13 W) microwave beam was gated[13] so that it remained "on" for only 3 s to maximize the enhancements while avoiding overheating. During the experiments the sample was cooled using a flow of nitrogen gas (20 °C, ~1.5 bar, ~30 L min^{-1}) directed around the sample tube. A relatively long recycling delay (30 s) was used to further limit the temperature rise during microwave on experiments.

Fig. 2 shows the NMR intensity build-up curves observed for $^{13}CCl_4$ and $^{13}CHCl_3$ as a function of irradiation time (microwave on-time, also referred to as gating time). The NMR peak intensities increase monoexponentially for both compounds, with build-up times of 0.70 ± 0.05 s for $^{13}CCl_4$ and 0.33 ± 0.05 s for $^{13}CHCl_3$. In the case of $^{13}CHCl_3$, the build-up time is very similar to the nuclear T_1 of 0.30 s, according to saturation recovery curves recorded at the same field, radical concentration and temperature (20 °C); by contrast, the nuclear T_1 of CCl_4 (3 s) under the same conditions is considerably longer than the build-up time. This discrepancy could be explained by the rise in temperature during the DNP build-up experiment compared to the temperature during the NMR T_1 measurements. Notice that the peaks exhibit a fair amount of variability in these build-ups. This can be attributed to instrumental instabilities derived primarily from variability in the cooling gas flow (hence the temperature), microwave source power, and sweep coil regulation. Similar sample conditions and measurement methods were used to study ^{13}C in deuterated chloroform and phenylacetylene-2-^{13}C; their measured steady-state enhancements are summarized in Table 1, and the ancillary NMR spectra are shown in ESI† Fig. SI-2 and SI-3. The errors reported in Table 1 are estimated from the signal-to-noise ratio observed in the spectra. In the case of chloroform, two peaks are observed due to the J-coupling between the labelled ^{13}C and the covalently bonded ^{1}H. The larger errors stem from the relative change in heights between the two peaks present in ^{13}C labelled chloroform (Fig. 1: without microwaves, both peaks are equal in intensity while the left peak is stronger with

Table 1 Enhancements for various ^{13}C labelled target molecules. The solvent was not labelled. A 10 mM TEMPO/*n*-pentane-d_{12} solvent mixture was used in all cases

Target molecule (% vol in solvent)	Enhancement peak height ratios	Enhancement peak area ratios
Carbon tetrachloride (9%)	21 ± 1	20 ± 1
Deuterated chloroform (7%)	52 ± 1	70 ± 2
Chloroform (1%)	70 ± 7	88 ± 2
Phenylacetylene-2-^{13}C (5%)	35 ± 6	33 ± 1
n-Pentane-d_{12} (solvent)	1 ± 0.05	1 ± 0.05

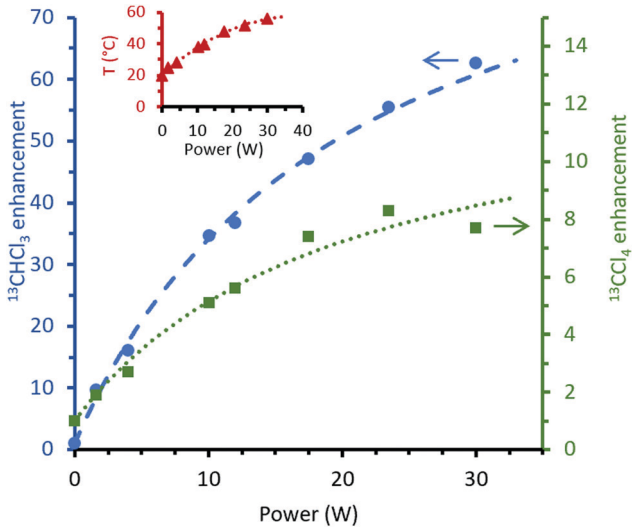

Fig. 3 ^{13}C enhancement for $^{13}CCl_4$ (green squares, arrow pointing to right scale) and $^{13}CHCl_3$ (blue dots, arrow pointing to left scale), as a function of microwave power. Respective enhancement models are also fit (dotted green line and dashed blue line). Inset: Sample temperature as function of microwave power (red triangles, the dotted red line is a guide to the eye). The same sample was used as in Fig. 1. Experimental parameters: 20 s relaxation delay (for both microwave on and off experiments), 16 and 2500 scans were averaged for on and off microwaves, respectively.

microwaves on). It should be noted that the difference in peak heights observed with microwaves on is explained by a temperature gradient (due to the probe geometry), combined with the temperature sensitivity of the chloroform ^{13}C chemical shift. If we were to add the instabilities observed at the longer gating times in Fig. 2, one would have to add ±10% to the errors on the enhancements. Note: the parameters A and B defined in Fig. 2 are used in the data analysis section.

The enhancements of $^{13}CCl_4$ and $^{13}CHCl_3$ were measured as a function of the applied microwave power (Fig. 3). The microwave gating time was chosen to be 0.5 s to limit the temperature rise, which reached 56 °C at the highest power setting (30 W); the sample temperature is shown in the inset to Fig. 3. The different gating times used explain the differences in enhancements at 13 W between Fig. 1 and 2. It should be noted that the sample tubes are sealed, allowing for some pressure to build-up, thus preventing the pentane solvent from evaporating during the DNP experiments.

In order to fit the measured power dependence of the enhancement (Fig. 3), we used the well-established Overhauser DNP model, according to which the enhancement ε is defined as[10]

$$\varepsilon = 1 - \rho f s \left|\frac{\gamma_e}{\gamma_n}\right|, \quad (1)$$

where ρ is the coupling factor, f the leakage factor, s the saturation factor, and γ_e, γ_n the gyromagnetic ratios of the electron and nucleus of interest, respectively ($|\gamma_e/\gamma_n| \approx 2600$ for 13C). The leakage factor $f = 1 - T_{1n}/T_{1n}^0$, can be estimated from measurements of the nuclear longitudinal relaxation in the presence (T_{1n}) and absence (T_{1n}^0) of radicals. In the cases of $^{13}CCl_4$ and $^{13}CHCl_3$ with 10 mM TEMPO, this leads to $f \approx 0.9$, which is consistent with previously published values.[9] The saturation factor is defined as:

$$s = \frac{1}{n}\frac{\gamma_e^2 B_1^2 T_{1e} T_{2e}}{1 + \gamma_e^2 B_1^2 T_{1e} T_{2e}}, \quad (2)$$

where n is the number of resolved hyperfine components of the EPR spectrum (3 for ^{14}N nitroxides), B_1 is the microwave magnetic field, and T_{1e} and T_{2e} are the electron longitudinal and transverse relaxation times, respectively. Eqn (2) becomes an inequality ($s \geq \ldots$) when the spectral diffusion is strong enough to reach the other ^{14}N hyperfine components besides the one used for excitation (in other words n could be less than the number of hyperfine components observed). 10 mM TEMPO in a low viscosity solvent[8] has 3 resolved hyperfine components, thus, using n = 3 would assume no spectral diffusion between the resolved hyperfine EPR spectral components. From Orlando *et al.*,[15] who found s = 0.53 in the case of strong spectral diffusion at 1.2 T using a fullerene functionalized TEMPO radical at 10 mM in CCl_4, one can calculate an effective $n \approx 2$. The average microwave B_1 field (in Tesla) can be calculated from the microwave beam power P in watts (see ESI† for details) as $B_1 = 3 \times 10^{-5} P^{1/2}$, for a beam size of 3 mm, as used when collimating it into the DNP sample tube. A correction term, one for each compound, needs to be introduced to account for the gating time (0.5 s in Fig. 3), being shorter than the steady state where the enhancement is fully built-up (above 1 s for $CHCl_3$ and several seconds for CCl_4). The correction terms are the ratios B/A, as indicated in Fig. 2. We obtained correction factors of 1.1× for $CHCl_3$ and 1.7× for CCl_4, to be used as multipliers in the enhancement models in Fig. 3. Using the numbers above for n, B_1 and f, and including the correction terms, fitting the data in Fig. 3 to eqn (1) and (2) leads to coupling factors of −0.11 for $^{13}CHCl_3$ and −0.018 for $^{13}CCl_4$, as well as $T_{1e}T_{2e} = 1.8 \times 10^{-15}$ s^2 for both compounds (using n = 3, would lead to higher coupling factors by 50%). This $T_{1e}T_{2e}$ product is reasonable: T_{1e} and T_{2e} are typically in the 10 to 100 ns range for solutions of radicals such as TEMPO at room temperature and high magnetic fields;[7,16] for example, Denysenkov *et al.*[16] reported a $T_{1e}T_{2e}$ product of 3.5×10^{-15} s^2 at 9.2 T. Ultimately we found a saturation factor, s, of 0.3 at 30 W (with n = 2). This is a reasonably high value considering that the electron relaxation rates are very short, and we are not using a microwave cavity (thus allowing for large sample volumes). While the leakage factor is essentially maximized in our experiments, the bulk of the limitation for maximum enhancements in liquid DNP at high field comes from the saturation and coupling factors. In particular, the saturation factor does have some room for improvement under our experimental conditions: an increase could be possible either by intensifying the microwave power or by using a radical with a single narrow EPR line. Liquid Overhauser DNP coupling factors have been mostly studied at lower fields,[10,17] including a −0.37 value at 3.35 T for $^{13}CHCl_3$; this is consistent with our coupling factor, as $|\rho|$ is expected to decrease towards zero with increasing magnetic field. Also consistent are theoretical models[18] for chloroform, which

predict coupling factors in the −0.22 to −0.075 range at 16.4 T. Recently Orlando *et al.*[15] have measured enhancements of 23 for CCl_4 and 17 for $CHCl_3$ at 14.1 T. These results are similar to what we observe for CCl_4 but differ for $CHCl_3$. This difference could arise from different sample preparations, from the instrumentation used and/or experimental designs. Coupling factors will be directly influenced by the temperature *via* changes in the correlation times.[19] While we assume that the temperature is constant throughout the experiments, we know that this is not the case; as shown in the inset to Fig. 3, for instance, the temperature rose from 20 to 56 °C upon applying the highest microwave power. In liquids, the viscosity will decrease by about 30% in this temperature range.[20] This will influence the correlation times and the various relaxation times (T_{1n}, T_{2n}, T_{1e}, and T_{2e}) and, thus, influence the coupling factors. Another difference could relate to the microwave powers delivered at the sample, which are not necessarily the same as the power delivered by the gyrotron. In our setup the microwave propagation system, including the quasi-optical bridge, was designed to minimize losses.[13] Furthermore, our solvents (pentane and carbon tetrachloride, which account for 99% of the sample volume in Fig. 3) were chosen to be essentially transparent to microwaves at 395 GHz.

It is also interesting to speculate on the origin of the different enhancements that we observe for the different compounds (Table 1). Since all experiments were performed under the same experimental conditions (radical identity, concentration, solvent, microwave power), it can be assumed that the saturation coefficients were the same for all samples studied. One can conclude that the leakage factor f was the same in all cases as well, as corroborated by the very similar enhancements measured for CCl_4 in the different samples (see ESI,† Fig. SI-2 and SI-3). Therefore, the main parameter left to explain the variation in enhancements between the different compounds is the coupling factor. The model developed by Abragam[19] and Hausser-Stehlik[21] predicts a coupling factor dependence on the correlation times and, specifically, shorter correlation times give larger coupling factors. It should be added that the dipolar coupling has not been considered in this analysis as it is very weak at low radical concentration[8] and high field.[22] Furthermore, ^{13}C coupling factors for CCl_4 and $CHCl_3$ at high field have been demonstrated to be mostly scalar contacts rather than dipolar.[23]

In summary, this work demonstrates that significant enhancements of up to 70× at 14.1 T can be imparted on ^{13}C NMR signals of liquids *via* the scalar DNP Overhauser mechanisms, with high resolution (0.1 ppm) and large sample volumes (100 μL) that are approaching values typical for standard liquid-state NMR spectroscopy. This is a step towards the use of DNP to boost traditional high-resolution liquid NMR sensitivity. The next challenge is to demonstrate ^{1}H liquid Overhauser DNP enhancements at high field, while maintaining high resolution and large volume. This will require further development in the area.

Conflicts of interest

There are no conflicts to declare.

Acknowledgements

This work was supported by the National Science Foundation (grants numbers CHE-1229170, CHE-1808660 and DMR-1644779) and the State of Florida. The authors thank B. Trociewitz, W. W. Brey, J. Mckay, F. Mentink-Vigier and J. R. Long for technical assistance and stimulating discussion.

Notes and references

1 A. W. Overhauser, *Phys. Rev.*, 1953, **92**, 411–415.
2 T. R. Carver and C. P. Slichter, *Phys. Rev.*, 1956, **102**, 975–980.
3 G. J. Gerfen, L. R. Becerra, D. A. Hall, R. G. Griffin, R. J. Temkin and D. J. Singel, *J. Chem. Phys.*, 1995, **102**, 9494–9497.
4 J. H. Ardenkjaer-Larsen, B. Fridlund, A. Gram, G. Hansson, L. Hansson, M. H. Lerche, R. Servin, M. Thaning and K. Golman, *Proc. Natl. Acad. Sci. U. S. A.*, 2003, **100**, 10158–10163.
5 N. M. Loening, M. Rosay, V. Weis and R. G. Griffin, *J. Am. Chem. Soc.*, 2002, **124**, 8808–8809.
6 V. Denysenkov, M. J. Prandolini, M. Gafurov, D. Sezer, B. Endeward and T. F. Prisner, *Phys. Chem. Chem. Phys.*, 2010, **12**, 5786–5790.
7 J. G. Krummenacker, V. Denysenkov and T. F. Prisner, *Appl. Magn. Reson.*, 2012, **43**, 139–146.
8 P. Neugebauer, J. G. Krummenacker, V. P. Denysenkov, C. Helmling, C. Luchinat, T. F. Prisner, G. Parigi and T. F. Prisner, *Phys. Chem. Chem. Phys.*, 2014, **16**, 18781–18787.
9 P. Neugebauer, J. G. Krummenacker, V. P. Denysenkov, G. Parigi, C. Luchinat and T. F. Prisner, *Phys. Chem. Chem. Phys.*, 2013, **15**, 6049.
10 G. Liu, M. Levien, N. Karschin, G. Parigi, C. Luchinat and M. Bennati, *Nat. Chem.*, 2017, 6–10.
11 S. G. J. van Meerten, M. C. D. Tayler, A. P. M. Kentgens and P. J. M. van Bentum, *J. Magn. Reson.*, 2016, **267**, 30–36.
12 D. Yoon, A. I. Dimitriadis, M. Soundararajan, C. Caspers, J. Genoud, S. Alberti, E. de Rijk and J. Ansermet, *Anal. Chem.*, 2018, **90**, 5620–5626.
13 T. Dubroca, A. N. Smith, K. J. Pike, S. Froud, R. Wylde, B. Trociewitz, J. McKay, F. Mentink-Vigier, J. van Tol, S. Wi, W. Brey, J. R. Long, L. Frydman and S. Hill, *J. Magn. Reson.*, 2018, **289**, 35–44.
14 N. Y. Tan, R. Li, P. Bräuer, C. D'Agostino, L. F. Gladden and J. A. Zeitler, *Phys. Chem. Chem. Phys.*, 2015, **17**, 5999–6008.
15 T. Orlando, R. Dervisoglu, M. Levien, I. Tkach, T. F. Prisner, L. B. Andreas, V. P. Denysenkov and M. Bennati, *Angew. Chem., Int. Ed.*, 2018, 1416–1420.
16 V. P. Denysenkov, M. J. Prandolini, A. Krahn, M. Gafurov, B. Endeward and T. F. Prisner, *Appl. Magn. Reson.*, 2008, **34**, 289–299.
17 X. Wang, W. C. Isley III, S. I. Salido, Z. Sun, L. Song, K. H. Tsai, C. J. Cramer and H. C. Dorn, *Chem. Sci.*, 2015, **6**, 6482–6495.

18 S. Kucuk and D. Sezer, *Phys. Chem. Chem. Phys.*, 2016, 9353–9357.
19 A. Abragam, *The Principles of Nuclear Magnetism*, Oxford University Press, London, 1961.
20 Kaye and Laby, National Physical Laboratory, http://www.kayelaby.npl.co.uk/general_physics/2_2/2_2_3.html.
21 K. H. Hausser and D. Stehlik, *Adv. Magn. Opt. Reson.*, 1968, **3**, 79–139.
22 M. Bennati, *Electron Paramagnetic Resonance*, RSC Publishing, Cambridge, UK, The Royal., 2010, vol. 22.
23 G. Parigi, E. Ravera, M. Bennati and C. Luchinat, *Mol. Phys.*, 2018, 1.